Simplified Interpretation of Transport in Disordered Inorganic Ion Conductors from Vacancy Dynamics

Heiko Lammert[1] and Andreas Heuer[2]

[1]*Center for Theoretical Biological Physics and Department of Physics, University of California, San Diego, 9500 Gilman Drive, La Jolla, California 92093-0374, USA*

[2]*Institut für Physikalische Chemie, Westfälische Wilhelms Universität Münster and Sonderforschungsbereich 458, Corrensstrasse 30, 48149 Münster, Germany*

(Received 28 September 2009; published 23 March 2010)

Ion transport in structurally disordered inorganic ion conductors can be interpreted as cation jumps between sites provided by the network. Because of the small number of vacant sites and strong intercationic Coulomb interaction, their dynamics is very complex. Based on molecular dynamics simulations we recast the ion dynamics via a sophisticated mapping procedure into the corresponding vacancy dynamics. Remarkably, in this framework, the transport can be interpreted to a very good approximation as a noninteracting single-particle processes. In particular, the macroscopic conductivity can be directly obtained from the local vacancy hopping rates.

DOI: 10.1103/PhysRevLett.104.125901 PACS numbers: 66.30.Dn, 02.70.Uu

The dynamics of ions in disordered inorganic ion-conductors is a complex multiparticle problem [1,2]. The ions' interaction with the network is fundamental: first, because it supplies a persistent disordered potential energy landscape for the cations [3] and second, because the local fluctuations of the network atoms are essential for promoting cationic jumps [4,5]. Naturally, beyond the dilute limit, the interaction among the mobile cations is a key element which has to be taken into account for the theoretical description [6,7]. A quantitative description of conductivity spectra was formulated considering correlated back jumps [8], and experimental studies of cooperativity effects, observed, e.g., as deviations from the Nernst-Einstein relation [9], are used to characterize possible conduction mechanisms [10,11]. A complete microscopic theory of the ion conduction is, however, not available by now, and, due to the complexity of the problem, it would be extremely difficult to formulate. Meanwhile, a lot of insight has be gained from the theoretical analysis of simplified cases like the random barrier or random energy models [12–14], where the dynamics of a single particle in a disordered energy landscape is discussed. It turns out that, e.g., the frequency dependence of the conductivity can be nicely reproduced from these models.

A different approach to gain knowledge about ion conductors is via molecular dynamics simulations [4,15–20]. From the trajectories, microscopic information about the underlying mechanisms is available. For example, it has been shown for lithium silicate systems that the lithium dynamics can be interpreted as hops between sites provided by the network [18,21,22]. More surprisingly, the number of sites is only slightly larger than the number of cations [20,22,23]. Thus, the ion dynamics is restricted by the fact that adjacent sites are not available. Based on these observations, it has been speculated that the multiparticle cation dynamics might be also interpreted as a single-particle vacancy dynamics [18,22,24]. The approach has been used to explain important experimental features such as the effect of pressure on the cationic transport [10], but a complete treatment of the conduction, as demonstrated for crystalline systems [25], here requires additional microscopic information.

The goal of this work is threefold. First, we introduce a intricate mapping procedure to identify the vacancy dynamics for a continuous system. This is a highly nontrivial problem, e.g., due to the finite duration of jumps, the existence of collective cationic jump processes, or the possibility of double occupancy of sites. In principle, however, each jump by an ion corresponds to an opposite jump by a vacancy, and vacancy trajectories can be reconstructed from their jumps [26]. Second, for the example of the lithium disilicate system $(Li_2O)2(SiO_2)$, we analyze in a quantitative way to which degree the vacancy and the cationic dynamics can be interpreted in a single-particle framework. We confirm the key hypothesis (H) that the vacancy dynamics is to a good approximation single-particle-like and thus corresponds to a simple Markovian hopping process in an underlying energy landscape. Third, we exploit this feature to successfully describe the conductivity as a simple random walk of independent vacancies, based on the local hopping rules as derived from the simulations.

For the molecular dynamics simulations, we use the force field introduced by Habasaki [27]. This system has already been characterized in previous work [15,17,22]. Our system contains 270 cations among 1215 atoms at experimental densities. Two independent runs were performed in the canonical ensemble, each for a 40 ns simulation time at $T = 850$ K. The identification of the sites has been performed according to the clustering algorithm in-

troduced in [22]. In total, we have found 294 (293) sites. Note that 234 (235) sites can be populated by two ions and 14 (15) sites by three ions.

A first interesting comparison between transport interpreted in terms of cation or vacancy hopping can be made for the dependence of the waiting time on the local energy. We have defined a site energy E_{tot} which gives the average potential energy of a cation populating a given site [28]. In the most simple case of a single particle in a random trap model, $\log\langle\tau\rangle$ is strictly correlated with E_{tot}. In the real system, one expects two types of deviations. First, due to additional fluctuations of, e.g., the local barriers, a weaker dependence on E_{tot} is expected. This effect may be similar in the cation as well as in the vacancy approach. Second, due to additional effects of multiparticle competition, the local population no longer follows the Fermi-distribution [28], implying that E_{tot} is less relevant for the characterization of the site occupation. In consequence, one also expects a further decrease of the correlation between $\log\langle\tau\rangle$ and E_{tot} in case of significant multiparticle effects. Indeed, we observed only a very weak dependence of $\log\langle\tau\rangle$ on E_{tot} [28]. Repeating this analysis now for the vacancies [29], one finds a much stronger correlation, (with a correlation coefficient of 0.56 instead of -0.18 for the ions), in support of (H).

Next, we compare the dynamic properties of the cations and the vacancies at the level of individual jumps and residences. An important observable is the local waiting time distribution $f_i(\tau)$ for site i, determined for the cation and the vacancy dynamics. As shown in previous work [22,30], there exist significant dynamic heterogeneities, i.e., slow and fast sites. Here, we focus on the distribution for a single site. In case of single-particle dynamics (cation or vacancy), $f_i(\tau)$ is exponential. In the multiparticle case, the situation is more complex. The jump probability at a given time not only depends on the height of the barriers but also on the availability of adjacent sites. The latter will fluctuate with time, giving rise to a fluctuating jump rate. In the extreme case, the rate can be as low as zero (if, in case of cations, all adjacent sites are populated or, in case of vacancies, empty). The size of the fluctuations, and thus the relevance of multiparticle effects, can be quantified by comparing the standard deviation σ of the waiting time distribution with its first moment $\langle\tau\rangle$ for each site. In case of an exponential distribution, both values should be identical whereas for a broadened waiting time distribution, one generally expects $\sigma/\langle\tau\rangle > 1$. The plot of $\sigma/\langle\tau\rangle$ against $\langle\tau\rangle$, evaluated for all sites, is shown in Fig. 1 for cation as well as for vacancy dynamics. The values of $\langle\tau\rangle$ themselves are shorter by nearly 2 orders of magnitude for vacancies than for ions, with medians of 1.2 and 110 ps. This difference already suggests that the vacancies will be more independent than the ions, where the lack of free sites often is limiting. For the ratio $\sigma/\langle\tau\rangle$, one clearly sees that the median is much closer to unity for vacancies (0.96) than for cations (1.7), again supporting (H).

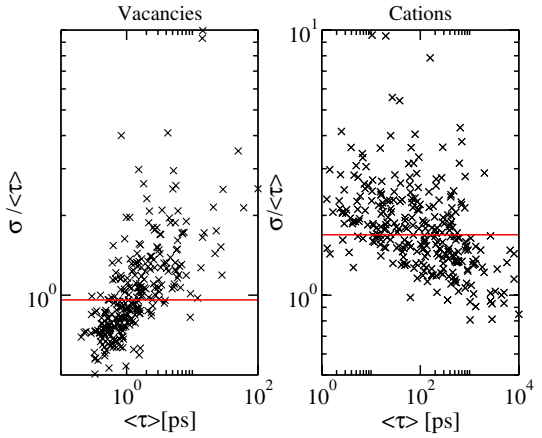

FIG. 1 (color online). The standard deviation of the waiting time distribution of vacancy and cation dynamics, respectively, normalized by the average waiting time. Each point reflects the properties of one site. Median values are included as lines.

The slight dependence of $\sigma/\langle\tau\rangle$ on $\langle\tau\rangle$ can be easily rationalized for the cations. Here, a large value of $\langle\tau\rangle$ implies that fluctuations in the populations of adjacent sites are on average faster than the site residence time. Thus, the escape process is mainly governed by an average rate with nearly exponential distribution. Correspondingly, the heterogeneities are most prominent for short $\langle\tau\rangle$.

The situation is more subtle for vacancies. The most prominent observation is the presence of sites with short $\langle\tau\rangle$ where $\sigma/\langle\tau\rangle$ is slightly smaller than unity. The very fast reoccupation of a vacated site by a cation suggests some aspects of cooperativity between the two jumps involved. This violates the assumption of a Markov process and may give rise to a narrower-than-exponential waiting time distribution.

For further investigations of correlated dynamics, we have assembled continuous vacancy trajectories from the individual jumps, explicitly considering the scenarios shown in Fig. 2. As a direct observation, this analysis shows that only 60 to 70% of the ion jumps in both simulation runs use existing vacancies, as in Figs. 2(a)–2(c). The remaining jumps are part of circular trajectories using a transient vacancy, which is created by the first jump and filled again by the last one. Most frequent are two-site exchange processes, shown in Fig. 2(d). More

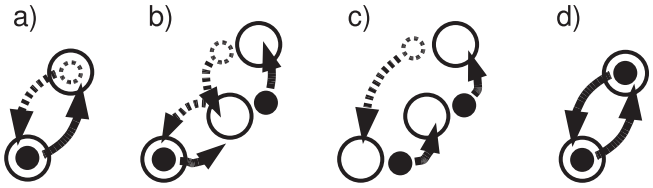

FIG. 2. Elements of the vacancy analysis: (a) An ion and a vacancy switch sites via corresponding jumps. (b) Sequential vacancy jumps may use different ions. (c) Simultaneous ion jumps form a cooperative vacancy jump. (d) Circular sequences of ion jumps create and use transient vacancies.

complex possibilities are discussed in the supplementary material [26]. All such circular processes eventually only permute the original configuration of ions. Therefore, they make no lasting contribution to charge transport.

After connecting single jumps into trajectories, as shown in Fig. 2(b), we have determined in general how often the jump of a cation is part of a larger cooperative sequence of simultaneous cation jumps, illustrated in Fig. 2(c), corresponding to a jump of the vacancy beyond the nearest-neighbor site. Interestingly, the number of longer sequences is in all cases very small; i.e., in 83% of all cases, only a single cation is involved, which corresponds to a nearest-neighbor jump of the vacancy. E.g., less than 1% of the sequences involve more than five ions. Thus, the effect of cooperativity for the analyzed temperature on the overall dynamics is small.

The probability for correlated back jumps by a single particle, p_{back}, is a third observable that allows us to judge the importance of interactions for the dynamics of cations and vacancies. Even for a simple single-particle trajectory in a disordered landscape, one expects correlated forward-backward jumps due to the presence of, e.g., a distribution of barrier heights [31]. Multiparticle effects increase the forward-backwards dynamics because some pathways are temporarily blocked due to the presence of other particles. To identify this additional multiparticle contribution to p_{back}, we have determined for every site i the probabilities $p_{ji}(i)$ and $p_{ij}(i)$ that a particle has jumped into i from neighbor j, and that it will next jump again into site j. In the single-particle limit, the probability for a correlated backward jump via i follows from simple statistical arguments and can be written as

$$p_{i,\mathrm{stat}} = \sum_j p_{ji}(i) p_{ij}(i). \tag{1}$$

The result is equally valid for both cations and vacancies because the values of $p_{ij}(i)$ and $p_{ji}(i)$ are simply exchanged between them. Their actual backward probabilities $p_{i,\mathrm{back}}$ in contrast can be different: If, after exchanging sites with an ion, the vacancy jumps on forward, the ion can still perform a back jump with its next jump, as soon as a vacancy becomes available again [32].

The comparison of the measured probability $p_{i,\mathrm{back}}$ with $p_{i,\mathrm{stat}}$ is shown in Fig. 3 for both ions and vacancies. One can clearly see that in the vacancy approach the distribution of p_{back} is much closer to the distribution of p_{stat} than in the cation approach, in particular, for large values of p_{back}. This is the third piece of independent information in favor of (H). Interestingly, for very small values of p_{back}, one can observe a significantly increased contribution for the vacancy approach. This reflects, at least partly, the presence of cooperative jumps where sites are definitely reoccupied by a different ion.

Probably the most essential dynamic observable for ion conductors is the conductivity, which characterizes the macroscopic transport. It can be derived from the center-of-mass (c.m.) dynamics via the mean-square displacement (MSD). In the present context, we are interested in the long-range transport related to the discrete jumps between the individual sites, and not in the vibrational contributions to the MSD that are also included in the continuous trajectories. We have thus mapped each cation position onto the (discrete) position of the corresponding site where the cation resides at that time [22]. Of course, this procedure does not modify the value of the dc conductivity. The resulting MSD of the c.m. is shown in Fig. 4.

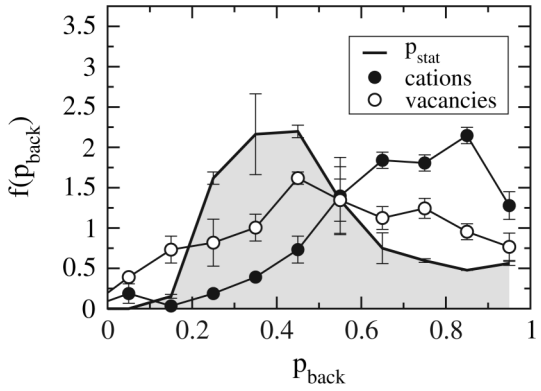

FIG. 3. The distribution of the backward jump probability p_{back} for three different cases: theoretical expectation p_{stat} in the single-particle limit and actual jumps of cations and vacancies, respectively.

While they make no permanent contribution to the ion transport, the observed circular dynamics of the transient vacancies also involve temporary displacements of ions. Their effect on the MSD has been subtracted to yield the contribution carried by permanent vacancies. As also shown in Fig. 4, in the diffusive regime this is practically identical with the total MSD. At the shortest times, however, the additional dynamics of the transient vacancies are responsible for $1/3$ of the c.m. MSD.

In case that the single-jump properties of the vacancies are strictly Markovian, the c.m. dynamics can be equiva-

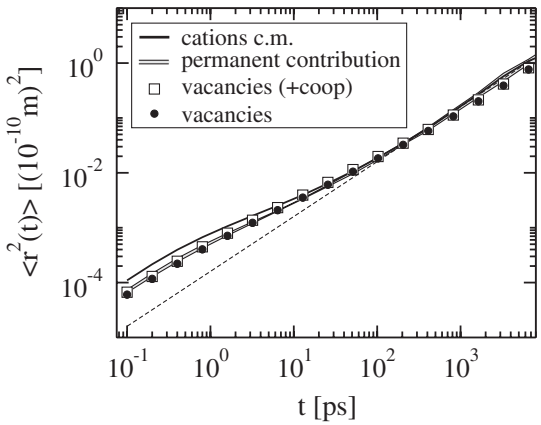

FIG. 4. Total mean-square displacement of the center-of-mass of the ions, and the contribution from permanent vacancies, ignoring transient ones. Furthermore, the MSD of independent vacancies, generated via Monte Carlo simulations with and without explicit inclusion of cooperative jumps is shown.

lently expressed in terms of a single-vacancy dynamics. Then, representative vacancy trajectories can be generated by Monte-Carlo (MC) simulations. The jump statistics for the MC simulations, and also for the previous analysis, were determined from the total set of jumps, including those of transient vacancies. While the transient vacancies are distinguished from permanent ones by their circular trajectories taken as a whole, differences are small at the level of single jumps and their statistical properties. Despite their share of up to 40% of the total jumps, the transient vacancies only add 5% new connections, mostly with very small weight. This indicates that the strongly correlated dynamics of the transient vacancies takes place on the same network of jump paths as the long-range transport of the ions through permanent vacancies, and it justifies our use of both contributions for an optimal description of that network. The relevant pieces of information, extracted from the simulations, are the average waiting times of the vacancies at each site, the probabilities $p_{ij}(i)$ to jump from site i to site j, and the explicit positions of the sites. On this basis, we have calculated the MSD of a single vacancy. For comparison with the c.m. data, the MSD has been additionally scaled by the number of vacancies, i.e., 24(23).

The very good agreement in Fig. 4 between the single-vacancy dynamics and the c.m. MSD due to the permanent vacancies is not further improved by explicit treatment of cooperative jump events, as their small number suggests. Geometrical factors can explain the observed Haven-Ratio smaller than unity in the absence of strong cooperativity [32]. The stability of the sites [23] and the weak temperature dependence of H_R [33,34] support a similar situation at lower temperature. Also, without correlations between distant ions, the separated vacancies must remain independent too, as our analysis assumes.

More frequent back jumps and therefore a stronger dispersion in the MSD are expected due to the increasing importance of disorder in the energy landscape. For the permanent vacancies, our method can directly capture this behavior; the excluded contribution to the MSD from temporary vacancies should remain limited at low temperature by the extra energy cost for their creation.

In summary, we have shown that the complex multiparticle ionic motion can be equivalently described as a (nearly) single-particle vacancy dynamics in a disordered energy landscape, including all the information about the complex Coulomb interaction. Since the number of vacancies is small compared to the number of cations also for other disordered ion conductors, this observation is expected to hold beyond the specific example of lithium disilicate. Thus, a minimal description using the simpler vacancy picture could form the core of a realistic model of disordered ion conductors.

We are grateful to Radha Banhatti for valuable discussions. This work was supported in part by Sonderforschungsbereich 458 and by the Center for Theoretical Biological Physics sponsored by the NSF (Grant No. PHY-0822283) with additional support from No. NSF-MCB-0543906.

[1] M. D. Ingram, Phys. Chem. Glasses **28**, 215 (1987).
[2] J. C. Dyre, P. Maass, B. Roling, and D. L. Sidebottom, Rep. Prog. Phys. **72**, 046501 (2009).
[3] C. A. Angell, Solid State Ionics **9–10**, 3 (1983).
[4] E. Sunyer, P. Jund, and R. Jullien, J. Phys. Condens. Matter **15**, S1659 (2003).
[5] M. Kunow and A. Heuer, Phys. Chem. Chem. Phys. **7**, 2131 (2005).
[6] P. Maass, J. Non-Cryst. Solids **255**, 35 (1999).
[7] B. Roling, Phys. Chem. Chem. Phys. **3**, 5093 (2001).
[8] K. Funke and R. D. Banhatti, Solid State Ionics **169**, 1 (2004).
[9] J. O. Isard, J. Non-Cryst. Solids **246**, 16 (1999).
[10] A. W. Imre, H. Staesche, M. D. Ingram, K. Funke, and H. Mehrer, J. Phys. Chem. B **111**, 5301 (2007).
[11] K. Funke, R. D. Banhatti, D. Laughman, M. Mutke, and M. D. Ingram, Eur. Phys. J. Special Topics **161**, 65 (2008).
[12] A. G. Hunt, J. Phys. Condens. Matter **3**, 7831 (1991).
[13] S. D. Baranovskii and H. Cordes, J. Chem. Phys. **111**, 7546 (1999).
[14] J. C. Dyre and T. B. Schrøder, Rev. Mod. Phys. **72**, 873 (2000).
[15] J. Habasaki, I. Okada, and Y. Hiwatari, J. Non-Cryst. Solids **183**, 12 (1995).
[16] J. Oviedo and J. F. Sanz, Phys. Rev. B **58**, 9047 (1998).
[17] R. D. Banhatti and A. Heuer, Phys. Chem. Chem. Phys. **3**, 5104 (2001).
[18] A. N. Cormack, J. Du, and T. R. Zeitler, Phys. Chem. Chem. Phys. **4**, 3193 (2002).
[19] J. Horbach, W. Kob, and K. Binder, Phys. Rev. Lett. **88**, 125502 (2002).
[20] M. Vogel, Phys. Rev. B **70**, 094302 (2004).
[21] S. Balasubramanian and K. J. Rao, J. Phys. Chem. **97**, 8835 (1993).
[22] H. Lammert, M. Kunow, and A. Heuer, Phys. Rev. Lett. **90**, 215901 (2003).
[23] J. Habasaki and Y. Hiwatari, Phys. Rev. B **69**, 144207 (2004).
[24] J. C. Dyre, J. Non-Cryst. Solids **324**, 192 (2003).
[25] M. Martin, J. Electroceram. **17**, 765 (2006).
[26] See supplementary material at http://link.aps.org/supplemental/10.1103/PhysRevLett.104.125901 for information about algorithm and mechanisms.
[27] J. Habasaki and I. Okada, Mol. Simul. **9**, 319 (1992).
[28] H. Lammert, R. D. Banhatti, and A. Heuer, J. Chem. Phys. **131**, 224708 (2009).
[29] See Fig. S1 in EPAPS Document No. http://link.aps.org/supplemental/10.1103/PhysRevLett.104.125901.
[30] J. Habasaki and Y. Hiwatari, Phys. Rev. E **59**, 6962 (1999).
[31] J. Kimball and L. Adams, Phys. Rev. B **18**, 5851 (1978).
[32] G. E. Murch, Solid State Ionics **7**, 177 (1982).
[33] A. Heuer, M. Kunow, M. Vogel, and R. D. Banhatti, Phys. Chem. Chem. Phys. **4**, 3185 (2002).
[34] C. Lim and D. E. Day, J. Am. Ceram. Soc. **60**, 198 (1977).